JOURNAL OF CATALYSIS 5, 484–493 (1966)

Organic Reactions Catalyzed by Crystalline Aluminosilicates

II. Alkylation Reactions: Mechanistic and Aging Considerations

P. B. VENUTO, L. A. HAMILTON, AND P. S. LANDIS

From the Applied Research & Development Division
and Central Research Division
Socony Mobil Oil Company, Inc.
Paulsboro and Princeton, New Jersey

Received Nobember 3, 1965; revised December 27, 1965

On the basis of product distributions, patterns of substrate reactivity, and promotion and deuterium tracer experiments, alkylation reactions catalyzed by acidic faujasites rare-earth–exchanged X and Y and hydrogen Y are defined as proceeding via carbonium-ion-type mechanisms. Sites active for alkylation in these three acidic faujasites are visualized as strongly acidic and ultimately protonic.

In alkylations with low molecular weight olefins, complex intracyrstalline polymerization–hydrogen transfer reactions of the olefin were shown to be responsible for catalyst aging.

INTRODUCTION

There are numerous recent reports of acid-catalyzed transformations utilizing crystalline aluminosilicates (*1–8*), and Hirschler's detection by ultraviolet spectroscopy in 1963 of the trityl carbonium ion from triphenylmethanol adsorbed on CaX zeolite (*9*) seemed eminently logical.

Shortly thereafter, however, the isolation and storage of stable free radicals on molecular sieves was reported, with clearly detectable ESR spectra arising from nitrogen dioxide adsorbed on Na– and Ca–X (*10*) and NF_2 radicals (from the equilibrium $N_2F_4 \rightleftharpoons 2\ NF_2$) on 5A, NaX, and CaX (*11*). Working with decationated zeolite Y, Stamires and Turkevich (*12*), by detecting a small population of adsorbed radical cations of triphenylamine and 1,1-diphenylethylene through their ESR spectra, demonstrated single electron transfer from organic molecule to electron-acceptor sites. Such electron-transfer processes were proposed for less polarizable molecules at higher temperatures in catalytic processes. Decationized Y zeolites have also shown catalytic activity in hydrogen–deuterium equilibration at 25°C (*13*).

The above facts, hinting at the complex multiplicity of reaction paths possible over crystalline aluminosilicates, warn of the dangers of over generalization. In the present paper, the mechanistic and aging patterns specific to alkylation are discussed, utilizing the primary data reported in Paper I (*14*) in this series, together with some additional experimental data.

EXPERIMENTAL

Catalysts. The rare earth X catalyst (REX) was prepared by exchanging Linde 13X with 5% mixed rare earth chloride ($RECl_3 \cdot 6\ H_2O$) solution until a sodium level of 0.58% by weight was obtained. A typical analysis of the rare earth mixture (as % wt oxide) employed in these exchanges is La_2O_3 (24.1), CeO_2 (48.0), Pr_6O_{11} (5.9), Nd_2O_3 (19.1), Sm_2O_3 (2.0), Gd_2O_3 (0.7), others (0.2). The rare earth Y catalyst (REY) was prepared similarly by base-exchanging a synthetic sodium Y aluminosilicate (NaY) with 5% $RECl_3 \cdot 6\ H_2O$ solution until a sodium level of 0.99% wt was obtained. The ammonium Y catalyst (NH_4Y) was obtained from a synthetic NaY zeolite by exchange with warm 10% aqueous ammonium chloride solution until a sodium level of 1.05% wt was obtained. Thermal deamination of NH_4Y gave hydrogen Y (HY) catalyst. All catalysts were binder-free and were pelletted, crushed, and sized to 8/14 mesh before activation. Detailed catalyst analyses and activation procedures, as well as general experimental and analytical techniques, have been reported earlier (*14*).

Infrared spectra of catalysts. Spectra were run as mulls (Fluorolube S, Hooker Electrochemical Co.) between sodium chloride plates. Catalyst, appropriately pretreated, was transferred without exposure to the atmosphere, to a dry box for mulling.

Treatment of REX catalyst with proton donors. A weighed sample of catalyst was calcined 3 hr in oxygen at 400°C in a tubular reactor previously described (*14*). The catalyst was then transferred (in a dry box) to the previously dried glass apparatus shown in Fig. 1. The stopcock was closed to the atmosphere, and the apparatus transferred to a vacuum system and evacuated (0.2 mm) for 0.5 hr. The flask was then sealed off from the vacuum, and promoter (1.85 meq/g catalyst) injected through the rubber septum at room temperature. A 100-μl syringe was used for water, while a 50-ml gas syringe was used for gaseous hydrogen halides. The apparatus was allowed to equilibrate overnight, after which time the pressure was usually less than 1 mm, indicating almost complete sorption of promoter by catalyst. The catalysts were then transferred (in a dry box) to a tubular reactor, and activity for benzene–ethylene alkylation determined.

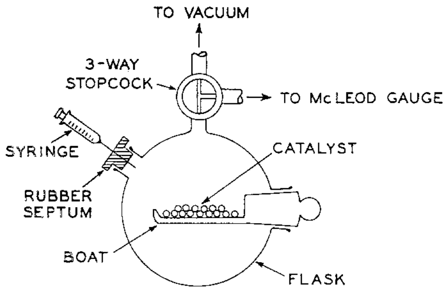

FIG. 1. Vapor-phase catalyst promotion apparatus.

Preparation of deuterated REX catalyst. REX catalyst (4.8 g) was calcined 3 hr at 500°C in oxygen in a tubular reactor. The catalyst bed was cooled to 100°C under a stream of dry nitrogen, and deuterium oxide (0.288 g, Matheson 99.5%) injected into the nitrogen carrier stream at the entrance of the hot (150°C), quartz-filled preheater. A moderate exotherm was observed when the gaseous deuterium oxide reached the catalyst bed. The reactor was then rapidly cooled and the catalyst transferred (in a dry box) to a dry ampoule, which was sealed under nitrogen with a serum cap and stored in a desiccator. Infrared (IR) examination of such a sample showed a broad envelope at 2597–2326 cm^{-1} (O–D stretching), which was almost completely absent in the catalysts after reaction.

Hexene-1 isomerization over deuterated REX. Hexene-1 (2.6 g, 4 ml) was added by hypodermic syringe in a dry box to the ampoule containing the deuterated catalyst described above. The catalyst darkened and heat was evolved. The ampoule was then frozen in liquid nitrogen and sealed. After heating at 64°C for 1.75 hr, the ampoule was opened and about 3 ml of pale yellow liquid was decanted and subjected to analysis. GLC analysis (mole % basis, silicone gum rubber on Chromosorb W) showed the presence of unreacted hexene-1 (19.0%), *trans*-hexene-2 and -3 (74.5%), hexene dimers (5.5%), and hexene trimers (1.0%). The total amount of hexene-1 converted to hexene isomers and polymer was about 82.3%. Table 1 shows the distribution of deuterium in the total liquid monoolefinic product. IR analysis of the product (neat, potassium bromide cell, 0.056 mm) showed the presence of a weak band at 2155 cm^{-1} (C–D stretching vibration in $-CHD-$ or $-CH_2D$).

Analysis of the organic matter entrapped within the pores of the REX catalyst was effected after dissolution of the inorganic skeleton of the catalyst. The discharged REX catalyst was dried (1.5 hr/25°C/0.5 mm) and dissolved by stirring with 100 ml of 2*N* HCl in the presence of 100 ml of chloroform for 0.5 hr. The organic layer was separated, and the aqueous-acid layer

TABLE 1

DISTRIBUTION OF DEUTERIUM IN C_6, C_{12}, AND C_{18} FRACTIONS OF MONOOLEFINIC REACTION PRODUCTS OF HEXENE-1 AND DEUTERATED REX CATALYST

Degree of deuteration	Mole % of isomer[a]		
	C_6	C_{12}	C_{18}
d_0	66.2	23.0	6.5
d_1	25.5	23.9	9.8
d_2	5.3	18.8	13.0
d_3	2.0	14.8	12.9
d_4	0.9	9.8	12.9
d_5	—	5.9	12.9
d_6	—	2.9	9.6
d_7	—	1.0	6.4
d_8	—	—	9.5
d_9	—	—	3.2
d_{10}	—	—	3.2
	99.9	100.0	99.9

[a] Mass spectroscopic analysis, 7 eV.

washed with chloroform. The two chloroform fractions were combined and dried over anhydrous sodium sulfate. The solvent was then removed *in vacuo* to give about 0.5 g of red-brown oil. GLC analysis (mole % basis) showed hexene dimers (67.1%), trimers (22.8%), tetramers (7.4%), and other higher polymers (2.7% based on pentamer). The IR spectrum (neat) showed a relatively intense aliphatic C–D stretch centered at 2143 cm^{-1}, characteristic of $-CHD-$ or $-CH_2D$. The complete absence of aromatics was shown by ultraviolet (UV) analysis.

Reaction of benzene and hexene-1 over deuterated REX. The above-described procedure for hexene-1 isomerization was followed, except that an equimolar mixture of benzene and hexene-1 was added to 1.4 times its weight of deuterated REX. The ampoule was heated for 1 hr at 80°C, then broken and the contents analyzed. GLC analysis showed that 33.2% of hexene-1 was converted to mono- and dihexylbenzenes (molar ratio 1.52:1). The C_{12} alkyl aromatics were almost exclusively 2- and 3-phenylhexane. About 22.2% of hexene-1 was converted to dimers and trimers (molar ratio 1.25:1), with the remainder either unreacted or isomerized to *trans*-2- and 3-hexenes. Table 2 shows the distribution of deuterium in the liquid C_{12} and C_{18} products. The IR spectrum (neat) of the product mixture showed a moderately intense band at 2165 cm^{-1} (aliphatic C–D stretch in $-CDH-$, $-CH_2D$, etc.); no aromatic C–D bands were detected.

TABLE 2

DISTRIBUTION OF DEUTERIUM IN LIQUID C_{12} AND C_{18} FRACTIONS OF REACTION PRODUCTS OF HEXENE-1 AND BENZENE OVER DEUTERATED REX CATALYST

Degree of deuteration	Mole % of isomer[a]			
	C_{12}		C_{18}	
	Monoolefin	Alkylbenzene	Monoolefin	Alkylbenzene
d_0	31.4	55.9	27.6	29.6
d_1	38.4	31.9	24.1	33.2
d_2	18.6	9.0	24.1	21.6
d_3	11.6	3.2	24.1	9.2
d_4	—	—	—	3.5
d_5	—	—	—	2.9
	100.0	100.0	99.9	100.0

[a] Mass spectroscopic analysis, 7 eV.

Reaction of ethylene and REX catalyst. REX (5.0 g), previously calcined 3 hr at 400°C in oxygen, was placed in a tubular glass reactor, which was then purged with nitrogen for 1.5 hr at 213°C. The nitrogen flow was shut off, and ethylene passed through (12 ml/min at 1 atm) continuously for 210 min. During this period, the catalyst color changed from pale yellow, through gray, to ochre-orange, and a "hot spot" moved through the catalyst bed. The effluent gas flow decreased to about 2 ml/min, indicating intracrystalline reaction, and after about 60 min, low molecular weight paraffin gases were evolved (Fig. 4, below). After about 3 hr, the intracrystalline reaction was complete, and the effluent gas consisted largely of ethylene. Gas analyses were by mass spectroscopy and GLC.

After termination of the run, the discharged catalyst showed a gain in weight of 18.8%, with C/H ratio of 0.68 for the entrapped organic matter. The catalyst was dissolved in 2*N* HCl, and the organic matter extracted in chloroform. The viscous, dark, organic extract was then analyzed by elution chromatography, GLC, elemental analysis, and spectroscopy (IR, UV, NMR, mass). Runs with ethylene were also made at 177°C (390 min), 149°C (345 min), 121°C (360 min), and 93°C (405 min) with similar workup (see Table 8 below).

RESULTS AND DISCUSSION

General Charcteristics of Acid-Zeolite-Catalyzed Alkylation Reactions

Earlier (*14*) it was reported that in typical alkylations of substituted benzenes, *ortho*:*para* orientation of substituents was usually observed, and that in alkylations with alkylating agents of three or more carbon atoms, the monoalkylate consisted of a mixture of isomers. Structurally, these isomers generally consisted of unbranched paraffin chains with the aryl residue attached at various secondary carbon atoms along the chain. Further, for a given aromatic, the temperature for appreciable reaction with different alkylating agents generally decreased, or, for a given temperature, the conversion of alkylating agent increased, in accord with the stability of the expected carbonium ion intermediate. Elimination reactions of alcohols and haloalkanes, and isomerization and polymerization of olefins (i.e., Tables 1 and 2) also accompanied their use as alkylating agents. Several other features of these alkylations are reported below.

Selectivity in electrophilic attack. In a competitive experiment between benzene and phenol for ethylene at 205°C (Table 3), a clear selectivity for the more reactive aromatic was shown, with $k(C_6H_5OH)/k(C_6H_6) = 6.95$. At 177°C under similar conditions, no ethylbenzene was formed.

Isomerization of aromatics. Conditions favorable for alkylation were also favorable for isomerization of di-(or poly-)substituted alkylbenzenes such as xylenes (Table 4) and for side-chain isomerization (*15*), dealkylation, and transalkylations of alkyl aromatics (Table 5).

Isomerization of paraffins. As shown in Table 6, isomerization and cracking of isobutane occurred under conditions favorable for alkylation of benzene with this paraffin.

Coke formation. Cokelike material was formed concomitant with these reactions via hydrogen-transfer reactions (*vide infra*).

Summary. The above features in the acid-faujasite–catalyzed reactions are typical of the patterns commonly reported (*16*) for alkylations with very strong protonic acids such as sulfuric, hydrofluoric, and promoted Lewis acids. The data further suggest the generation, within the intrazeolitic environment, of selective electrophiles which then attack the aromatic nuclei.

TABLE 3
PHENOL–BENZENE ALKYLATION WITH ETHYLENE OVER REX CATALYST AT 204°C[a]

Product	Mole %[b]
Benzene	33.80
Ethylbenzene	0.96
Phenol	54.50
Ethylphenol	10.43
Diethylphenols	0.31
	100.00

[a] 400 psig; LHSV 4; phenol: benzene (molar ratio), 1.66; total aromatic/ethylene (molar ratio), 5.

[b] Analysis of sample after 2 hr on stream.

TABLE 4
o-XYLENE ISOMERIZATION[a] OVER REX CATALYST

	177°C	204°C
% Conversion, *o*-Xylene[b]		
Initial	30	70
Aged	43 (8 Hr)	50 (50 Hr)
Products (Mole %)[c]		
m- and *p*-Xylene	68.4	78.0
Toluene	17.4	12.1
Trimethylbenzenes	14.2	9.9[d]
	100.0	100.0

[a] LHSV 0.25; 400 psig; aging was very severe at 1 atm.

[b] To all other products.

[c] Analyses on 8 hr (177°C) and 50 hr (204°C) samples.

[d] Very small amounts of benzene and higher polymethylbenzenes formed.

TABLE 5

TRANSFORMATIONS OF *sec*-BUTYLBENZENE OVER REX CATALYST[a]

A. Products	Mole %
Benzene	34.4
Butylbenzenes	59.9
Dibutylbenzenes	5.6
	99.9
B. Fate of *sec*-Butylbenzene	**Mole %**
Transalkylation	11.2
Dealkylation[b]	28.8
Isomerized or unreacted	60.0
	100.0
C. *sec*-Butyl groups in total product	**%**
isomerized to *iso*-butyl[c]	10

[a] 200°C, LHSV 4.20, atmospheric pressure, 30-min sample.

[b] Calculated from moles of benzene not required for transalkylation; butene peak observed on gas chromatograph.

[c] No other butylbenzene isomers observed (GLC); % isobutylbenzene in binary mixture with *sec*-butylbenzene determined by infrared (ref. *15*).

TABLE 6

REACTION OF ISOBUTANE OVER REX CATALYST[a]

Temperature (°C)	Mole % cracked or isomerized[b]
149	2.5
204	3.4
260	10.7
316	30.1
371[c]	52.2
427	62.0

[a] At atmospheric pressure and 25°C, 0.015 mole isobutane/g catalyst/hr passed over catalyst.

[b] Propane and *n*-butane were major products.

[c] Slight alkylation of benzene with isobutane occurs at this temperature.

Qualitative Visualization of Intrazeolitic Alkylation Process

The sites active in *alkylation* in the acid faujasites REX, REY, and HY are visualized as very strongly acidic and ultimately, as protonic acids. Supporting evidence is given below.

Strength of Acid Sites

At an early date, Pauling observed that an aluminum tetrahedron with corners shared with silicon tetrahedra was similar to the perchlorate ion, and that the acid obtained by replacing the potassium cation of an aluminosilicate (mica) by hydrogen ion should be very strong (*17*). In fact, the acidity of silica-alumina itself has been quantitatively related to that of 90% sulfuric acid (*18*). The recent work of Pickert and co-workers (*6*) on carboniogenesis in alkali- and alkaline-earth–exchanged Y-type faujasites clearly focuses on the role of the zeolite cations, with their powerful surrounding electrostatic fields, in inducing acid catalysis. Such trends toward strong acidity would be even more intensified in faujasites (REX, REY) exchanged with smaller, high charge density rare earth cations. Thus, we have observed (*14*) that for the same reactants, the acidic faujasites, with their order and rigidity (*6*), catalyzed alkylation at significantly lower temperatures than did amorphous silica-aluminas.

It was consistently observed, however, that for the same reactants, catalysis by the acidic faujasites occurred at significantly higher temperatures than with the "conventional" strong acids, sulfuric, hydrofluoric, promoted aluminum chloride, etc. In the zeolite there is a combination of driving forces, arising from its peculiar structure (*6, 19–24*), that tend toward condensation, strong adsorption, and generally decreased mobility of sorbed species, at least at low temperatures. If it is assumed that the acid faujasites are very strong acids, it seems reasonable to relate higher reaction temperatures to the additional energy barriers and entropy requirements imposed by mass transport, diffusion, sorption–desorption, etc., within the narrow, polar, rigid zeolite channel system. It further seems probable that such factors would be operative to some extent at the temperatures of most of these alkylation reactions.

Evidence for Protonic Sites

Enhancement of reaction rate or conversion upon introduction of a proton donor in an acid-catalyzed reaction strongly suggests a role for protons in the transformation. Just such a promotion effect is shown for the alkylation of benzene with ethylene, when REX catalyst (previously calcined at 400°C) was treated with 1.85 meq/g of water, hydrogen chloride, or hydrogen bromide immediately prior to reaction (Fig. 2). Conversely, the decrease in benzene–ethylene alkylation activity observed earlier (*14*) when REX and REY were precalcined at higher temperatures, probably reflects the loss of protons through dehydration. A similar promoting role for water has been reported for cyclopropane cracking over NaX (*1*), *tert*-butanol dehydration over CaX (*8*), and for numerous reactions over silica-alumina (*16*).

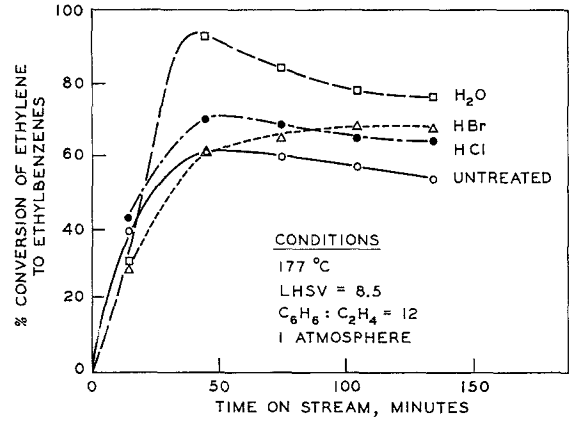

FIG. 2. Effect of proton donors on ethylene–benzene alkylation activity of REX catalyst.

Recently, Bertsch and Habgood (*25*) detected infrared OH-stretching vibrations in NaX-water systems, suggesting isolated water molecules adsorbed simultaneously by an ion–dipole interaction with the exchangeable cation and by hydrogen bonding of one of the hydrogens to lattice oxygen. In an extension of such reasoning, Hirschler (*9*) suggested that the polarizing action of the cation fields in Na– or Ca–X zeolites tended to make acidic the proton of a hydroxyl group attached to an adjacent lattice atom, or of a water molecule solvating the cation itself.

Sites active for alkylation in REX and REY may thus arise through an essentially reversible transfer of a proton from a residual, strongly held water molecule, either solvating the rare earth cation, or under the influence of its powerful fields, to oxygen of the associated AlO_4 tetrahedron. Realizing that every cationic positive charge must be balanced by an equivalent lattice negative charge, these events are visualized as follows:

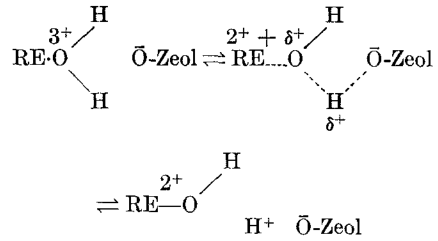

The formation of a proton-containing "HY" with an associated infrared OH band at 3570 cm^{-1} was postulated earlier by Rabo *et al.* (*26*). These workers also noted the instability of the protonic form at higher temperatures. Under our defined (*14*) conditions of thermal deamination of NH_4Y (I) in oxygen, the generation of protonic sites is visualized as shown in Eq. (1). The HY catalyst so obtained shows a single, intense infrared OH band at 3570 cm^{-1} [others (*27*) have reported two bands at 3660 and 3570 cm^{-1} in similar HY zeolites], and probably would be best represented by (III). It seems likely, however, that the HY site active in alkylation would more likely resemble the classical Bronsted acid (II), which might be present in significant con-

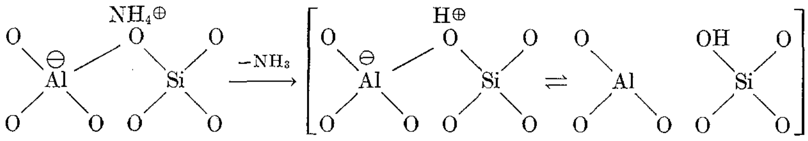

(I) (II) (III) (1)

centration at actual *reaction temperatures* as proposed by Hall and co-workers (*27*). The HY used in the present work is further defined as not having undergone extensive dehydroxylation (*27*) or decationation (*12*), a proton-removing process stoichiometrically involving the loss of 1 mole of water per pair of AlO_4 tetrahedra.

General Mechanistic Pathways

The reaction of 1-hexene and benzene at 80°C over deuterated REX (Table 2) serves as a convenient model for a visualization of the acid-faujasite–catalyzed alkylation process.

After initial adsorption of the olefin [Eq. (2)], transfer of a deuteron (D^+) from catalyst oxygen to organic carbon (as $-CH_2D$ or $-CHD$ groups) to form an electrophilic species, (V)–(VI), is proposed.

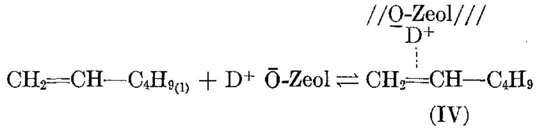

$$CH_2{=}CH{-}C_4H_{9(l)} + D^+\ \bar{O}\text{-Zeol} \rightleftharpoons \underset{(IV)}{\overset{\overset{//\underline{O}\text{-Zeol}///}{D^+}}{CH_2{=}CH{-}C_4H_9}} \tag{2}$$

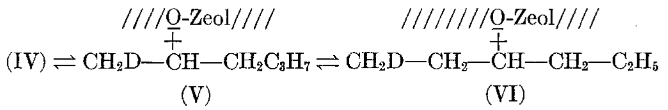

$$(IV) \rightleftharpoons \underset{(V)}{\overset{////\underline{O}\text{-Zeol}////}{CH_2D{-}\overset{+}{C}H{-}CH_2C_3H_7}} \rightleftharpoons \underset{(VI)}{\overset{///////\underline{O}\text{-Zeol}////}{CH_2D{-}CH_2{-}\overset{+}{C}H{-}CH_2{-}C_2H_5}} \tag{3}$$

The observed product distributions and deuterium concentrations (Tables 1 and 2) suggest that the equilibrations represented in Eqs. (2) and (3) must be rapid, relative to alkylation.

For the alkylation step, a Rideal-like process appears to be operative, with attack by benzene on adsorbed electrophile [Eq. (4)] to form 2- and 3-phenylhexane, (VII) and (VIII). Similarly, attack of hexene on adsorbed C_6 electrophile with subsequent elimination would generate hexene polymers. Associated with the alkylation and elimination reactions is the donation of a proton from the organic molecule to the catalyst surface.

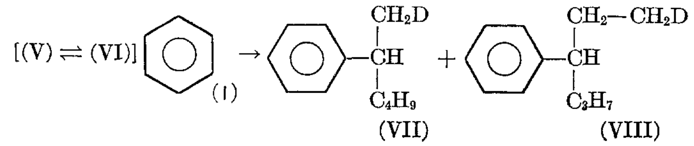

(VII) (VIII) (4)

It is certain that aromatics are adsorbed on certain zeolite sites, and indeed may even compete with olefins for them. However, those aromatics that attack adsorbed electrophiles (and hence are alkylated) are almost certainly only weakly adsorbed, or behave more liquid or gaslike in the intrazeolitic environment. An aromatic adsorbed strongly enough to have donated significant ring π-electron density to an electron-withdrawing site, either as π-charge drift or actual electron transfer, would be expected to have some degree of positive charge. As such, it would not be expected to attack positively charged electrophiles, since significant Coulombic repulsive forces would be encountered. Hence, a Rideal-like pattern is proposed.

Alkylations with *n*-alcohols and *n*-haloalkanes probably proceed analogously to those with olefins. However, as suggested in Table 7 for the alkylation of benzene with *n*-butanol and 1-butene, larger amounts of *n*-alkyl aromatics are formed. A small amount of *n*-butylbenzene was observed with 1-butene as alkylating agent, suggesting

TABLE 7
ALKYLATION OF BENZENE WITH 1-BUTENE AND *n*-BUTANOL OVER REX CATALYST[a]

	150°C		200°C	
	n-Butanol	1-Butene	*n*-Butanol	1-Butene
% Conversion[b]	15.9	78.2	85.5	83.7
Molar ratio, mono-/dibutylbenzene	3.28	19.1	21.5	11.1
Products (Mole-%)				
Toluene	Tr	2.7	1.5	7.7
Ethylbenzene	0.4	1.9	1.5	4.9
Cumene	Tr	0.4	Tr	1.5
n-Propylbenzene	Nil	0.4	Tr	0.9
tert-Butylbenzene[c]	Nil	Nil	Nil	Nil
sec-Butylbenzene	74.0	76.6	78.2	58.2
Isobutylbenzene[d]	Nil	13.1	12.8	19.4
n-Butylbenzene	2.3	0.2	1.5	0.4
Di- and tributylbenzene[e]	23.3	4.7	4.3	7.0
	100.0	100.0	99.8	100.0

[a] LHSV 4.20; atmospheric pressure; benzene/alkylating agent (molar) ratio 5; 30-min samples.
[b] Alkylating agent to alkyl aromatics (molar).
[c] Looked for at high sensitivity with large sample.
[d] Determined by infrared (ref. *15*).
[e] Traces of tributylbenzene also formed.

that small amounts of primary carbonium ion existed in the equilibration of adsorbed 1-butene. The larger amounts of *n*-alkylate observed with *n*-butanol, however, probably arise via concerted processes such as (IX).

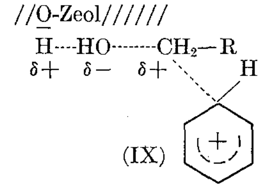

(IX)

The skeletally rearranged products shown in Table 7 are attributed to side-chain isomerization of product aryl alkanes (see Table 5).

The atmospheric pressure phenol ethylation data shown in Fig. 3 may be an example where elimination precedes or accompanies alkylation. The sharp increases in alkylation rate with ethyl chloride and ethanol coincide closely with the temperatures where smooth dehydrochlorination and dehydration, respectively, occur for the individual alkylating agents.

Catalyst Aging Pathways

In most of the continuous-flow alkylation reactions catalyzed by crystalline aluminosilicates, high initial conversions of reactants were obtained, with subsequent decreases in conversion with time. This catalyst aging results from blocking or obliteration of

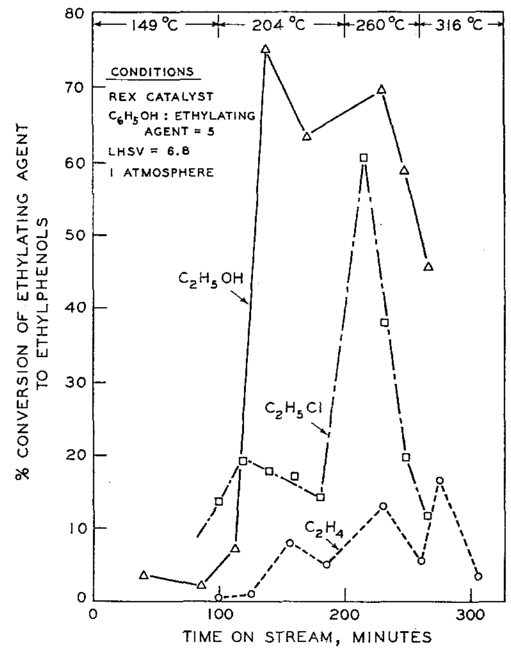

FIG. 3. Comparative phenol ethylations: effect of structure of alkylating agent.

TABLE 8
VARIATIONS IN PRODUCT DISTRIBUTION WITH TEMPERATURE FOR REACTION OF ETHYLENE WITH REX

Temperature (°C)	Major products	
	Intracrystalline	Gaseous
93	Liquid aliphatic polymer	Nil
121	Mixed aliphatic and aromatic polymer	Paraffins (traces)
149	Largely aromatics, small amounts aliphatic polymer	Paraffins (small amounts)
177	Exclusively aromatics	Paraffins (large amounts)
213	Exclusively aromatics[a]	Paraffins (large amounts)[b]

[a] 23% of alkylbenzenes (C_{15} and C_{16} predominant), at least 5% alkylnaphthalenes (C_{18}, C_{17}, C_{20} most prominent), with the remainder consisting of a complex mixture (average molecular weight 490 by vapor-pressure lowering) of alkylated polycyclic aromatics and their partially dehydrogenated analogs.

[b] Mixtures of paraffins similar to those shown in Fig. 4 were observed in the gaseous effluents when REX was exposed to propylene or 1-butene at 213°C, and when HY was exposed to ethylene at 213°C.

active sites by localized polymeric organic matter. With low molecular weight (C_2–C_4) olefin alkylating agents, or their alcohol and haloalkane precursors, and a simple aromatic such as benzene, most of the catalyst aging could be attributed to complex secondary reactions of the olefin with the catalyst. The reaction of ethylene alone with REX catalyst was studied in detail as typical of these interactions. The variation in product distributions for several such reactions at different temperatures is outlined in Table 8.

When ethylene was passed over REX at 213°C, a steady evolution of low molecular weight gaseous alkanes was observed (Fig. 4), but no liquid product was formed. When the inorganic catalyst skeleton was dissolved away after the reaction, a complex mixture of highly alkylated entrapped aromatics (Table 8) was revealed. The data in Table 8 and Fig. 4 suggest a complex series of reactions initially involving acid-catalyzed polymerization of ethylene to low molecular weight aliphatic polymer. Subsequent intermolecular hydrogen-transfer and dehydrogenation–cyclization reactions, accompanied by skeletal isomerization and cracking, result in the extrusion of low molecular weight alkanes, coupled with a buildup of bulky, hydrogen-deficient aromatics, which cannot diffuse out, either for steric reasons, or from powerful attractive interactions with the lattice. These species increase in molecular weight and carbon:hydrogen ratio, ultimately forming three-dimensional carbonaceous residues.

Mixtures of branched aliphatics and alkyl aromatics within the pores of CaA zeolite after dodecane cracking (*28*) and aromatics derived from secondary olefin reaction in hexadecane cracking over silica-alumina

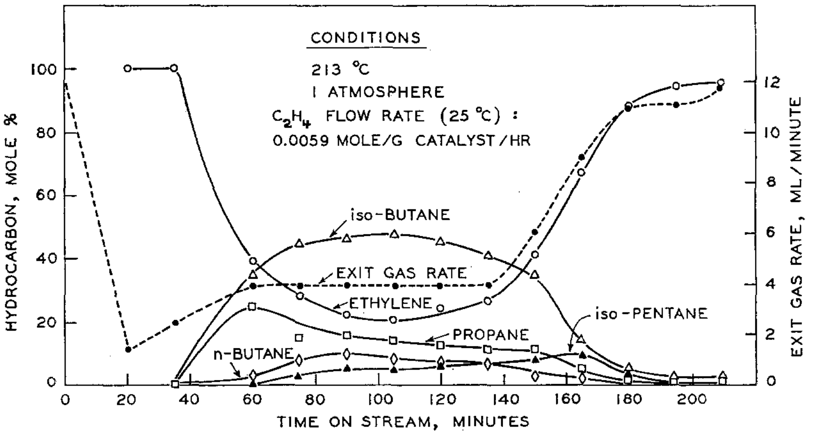

FIG. 4. Effluent gas analysis, ethylene–REX reaction.

(*29, 30*) have also been reported. Somewhat similar hydrogen-transfer reactions have been reported over silica-alumina in propylene polymerization (*31*) and in ethylene polymerization at low temperatures over promoted aluminum chloride (*32*).

Side reactions of other reactants, notably aromatics such as naphthalene and thiophene, or alcohols such as methanol, were also associated with rapid catalyst aging, although the pathways are less clear.

Acknowledgments

We wish to thank Mr. F. E. Harvey and Mr. R. M. Buckingham for their excellent technical assistance, and Prof. G. A. Russell of Iowa State University, Prof. L. S. Bartell of the University of Michigan, and Dr. R. L. Gorring of Socony Mobil for very helpful discussions.

References

1. Bassett, D. W., and Habgood, H. W., *J. Phys. Chem.* **64**, 769 (1960).
2. Keough, A. H., and Sand, L. B., *J. Am. Chem. Soc.* **83**, 3536 (1961).
3. Weisz, P. B., Frilette, V. J., Maatman, R. W., and Mower, E. B., *J. Catalysis* **1**, 307 (1962).
4. Norton, C. J., *Chem. and Ind.*, p. 258 (1962).
5. Mattox, W. J., British Patent 932,074, July 24, 1963.
6. Pickert, P. E., Rabo, J. A., Dempsey, E., and Shomaker, V., *Proc. Intern. Congr. Catalysis, 3rd, Amsterdam, 1964* **1**, 714 (Wiley, New York, 1965).
7. Fleck, R. N., Wight, C. G., and Wasley, W. L., U. S. Patent 3,132,186, May 5, 1964.
8. Gourisetti, B., Cosyns, J., and Leprince, P., *Compt. Rend.* **258**, 4547 (1964).
9. Hirschler, A. E., *J. Catalysis* **2**, 428 (1963).
10. Colburn, C. B., Ettinger, R., and Johnson, F. A., *Inorg. Chem.* **2**, 1305 (1963).
11. Colburn, C. B., Ettinger, R., and Johnson, F. A., *Inorg. Chem.* **3**, 455 (1964).
12. Stamires, D. N., and Turkevich, J., *J. Am. Chem. Soc.* **86**, 749 (1964).
13. Turkevich, J., Nozaki, F., and Stamires, D., *Proc. Intern. Congr. Catalysis, 3rd, Amsterdam, 1964* **1**, 586 (Wiley, New York, 1965).
14. Venuto, P. B., Hamilton, L. A., Landis, P. S., and Wise, J. J., *J. Catalysis* **5**, 81 (1966).
15. Roberts, R. M., and Shiengthong, D., *J. Am. Chem. Soc.* **82**, 732 (1960).
16. Patinken, S. H., and Friedman, B. S., *in* "Friedel-Crafts and Related Reactions" (G. A. Ohah, ed.), Vol. II, Part I, p. 31. Interscience, New York, 1964.
17. Pauling, L., "The Nature of the Chemical Bond," p. 558. Cornell Univ. Press, Ithaca, New York, 1960.
18. Benesi, H. A., *J. Am. Chem. Soc.* **78**, 5490 (1956).
19. Barrer, R. M., and Bratt, G. C., *J. Phys. Chem. Solids* **12**, 146 (1959).
20. Barrer, R. M., and Sutherland, J. W., *Proc. Roy. Soc.* (*London*) **237**, 439 (1956).
21. Barrer, R. M., Bultitude, F. W., and Sutherland, J. W., *Trans. Faraday Soc.* **53**, 1111 (1957).
22. Barrer, R. M., and Bratt, G. C., *J. Phys. Chem. Solids* **12**, 130 (1959).
23. Barrer, R. M., and Gibbons, R. M., *Trans. Faraday Soc.* **59**, 2569 (1963).
24. Habgood, H. W., *Can. J. Chem.* **36**, 1384 (1958).
25. Bertsch, L., and Habgood, H. W., *J. Phys. Chem.* **67**, 1621 (1963).
26. Rabo, J. A., Pickert, P. E., Stamires, D. N., and Boyle, J. E., *Actes Congr. Intern. Catalyse, 2^e, Paris, 1960* **2**, 2055 (Editions Technip, Paris, 1961).
27. Uytterhoeven, J. B., Christner, L. G., and Hall, W. K., *J. Phys. Chem.* **69**, 2117 (1965).
28. Galich, P. N., Gutyrya, A. A., Gutyrya, V. S., and Neimark, I. E., *Proc. Acad. Sci. U.S.S.R.* **144**, 349 (1962).
29. Van Hook, W. A., and Emmett, P. H., *J. Am. Chem. Soc.* **84**, 4421 (1962).
30. Hightower, J. W., and Emmett, P. H., *J. Am. Chem. Soc.* **87**, 939 (1965).
31. Shepard, F. E., Rooney, J. J., and Kemball, C., *J. Catalysis* **1**, 379 (1962).
32. Thomas, C. A., "Anhydrous Aluminum Chloride in Organic Chemistry," p. 798. Reinhold, New York, 1941.